

ZmMPK17, a novel maize group D MAP kinase gene, is involved in multiple stress responses

Jiaowen Pan · Maoying Zhang · Xiangpei Kong ·
Xin Xing · Yukun Liu · Yan Zhou ·
Yang Liu · Liping Sun · Dequan Li

Received: 26 July 2011 / Accepted: 19 August 2011 / Published online: 18 October 2011
© Springer-Verlag 2011

Abstract Plant mitogen-activated protein kinase (MAPK) cascades play a pivotal role in a range of biotic and abiotic stress responses. In this study, we isolated a novel group D MAPK gene, *ZmMPK17*, from maize (*Zea mays* L.). *ZmMPK17* is localized mainly to the nucleus and its C-terminal domain extension is believed to be essential for this. Northern-blot analysis indicated that *ZmMPK17* transcription is involved in response to exogenous signaling molecules such as abscisic acid, hydrogen peroxide, salicylic acid, jasmonic acid and ethylene and induced by low temperature and osmotic stress. Hydrogen peroxide and Ca^{2+} mediate PEG-induced downregulation of *ZmMPK17* at transcription level and Ca^{2+} also mediates low temperature-induced expression of *ZmMPK17*. Overexpression of *ZmMPK17* in tobacco (*Nicotonia tabaccum*) accumulated less reactive oxygen species under osmotic stress by affecting antioxidant defense systems. Transgenic tobacco exhibited enhanced tolerance to cold by means of an increased germination rate, and increased proline and soluble sugar levels relative to control plants. The transcription levels of *NtERD10* genes were higher in *ZmMPK17*-overexpressing lines than in control plants under cold and osmotic stress conditions. *ZmMPK17*-overexpressing plants displayed enhanced resistance to viral pathogens, and the expression of the pathogenesis-related gene *PR1a* was significantly increased,

indicating that *ZmMPK17* might be involved in SA-mediated pathogen defense-signaling pathways.

Keywords Low temperature · MAPK · Osmotic stress · Reactive oxygen species · Viral resistance · *ZmMPK17*

Abbreviations

ABA	Abscisic acid
APX	Ascorbate peroxidase
CaMV	Cauliflower mosaic virus
CAT	Catalase
CD	C-terminal domain extension
DMTU	Dimethylthiourea
DAB	3,3'-Diaminobenzidine
ELISA	Enzyme-linked immunosorbent assay
GFP	Green fluorescent protein
H_2O_2	Hydrogen peroxide
JA	Jasmonic acid
MAPK	Mitogen-activated protein kinase
NBT	Nitroblue tetrazolium
POD	Peroxidase
ROS	Reactive oxygen species
SA	Salicylic acid
SOD	Superoxide dismutase

J. Pan · M. Zhang · X. Kong · X. Xing · Y. Liu · Y. Zhou ·
Y. Liu · D. Li (✉)

State Key Laboratory of Crop Biology,
Shandong Key Laboratory of Crop Biology,
College of Life Sciences, Shandong Agricultural University,
61 Dai Zong Street, Tai'an 271018, Shandong, China
e-mail: dqli@sdau.edu.cn

L. Sun
Taishan Medical University, Tai'an 271018, Shandong, China

Introduction

To cope with the limitations of a sessile lifestyle, plants show a great ability to adapt their metabolism to rapid changes in the environment. They are equipped with complex processes, such as the perception and transmission of stress stimuli. One of the universal signaling modules that conveys perceived external stimuli to the nucleus is the

mitogen-activated protein kinase (MAPK) cascade (Tena et al. 2001). The MAPK cascade is evolutionarily conserved among the eukaryotes and typically consists of three types of protein kinases, MAPK, MAPK kinase (MAPKK), and MAPKK kinase (MAPKKK). MAPKKK phosphorylates a serine or threonine residue on a MAPKK, which in turn activates a MAPK, the last protein in the cascade. MAPKs are activated by the dual phosphorylation of threonine and tyrosine residues by MAPKK. The activated MAPK causes the phosphorylation of transcription factors and other signaling components that regulate the expression of downstream genes (MAPK Group 2002). Molecular and biochemical studies have revealed that MAPKs play important roles not only in response to a broad variety of biotic and abiotic stresses such as wounding, pathogen infection, temperature, drought and salinity, but also in the signaling of plant hormones and in processes involved in plant growth and development (Mishra et al. 2006; Colcombet and Hirt 2008; Pitzschke et al. 2009).

Since the first plant MAPK, *MsERK1* in alfalfa, was found (Duerr et al. 1993), MAPK genes have been identified and explored by both genetic and biochemical approaches. In tobacco (*Nicotiana tabacum*), two MAPKs, SIPK and WIPK, were shown to be activated by both various pathogen-related signals and diverse abiotic stresses (Zhang et al. 1998; Seo et al. 1999). Orthologs of SIPK and WIPK in *Arabidopsis* (AtMPK6 and AtMPK3) and alfalfa (*Medicago sativa*; SIMK and SAMK) are the best studied MAPKs (Rodriguez et al. 2010). Cold/salt stress induced the most complete MAPK cascade: the MEKK1–MKK2–MPK4 cascade (Teige et al. 2004). O₃ was shown to activate MPK3 and MPK6 through the production of reactive oxygen species (ROS) (Ahlfors et al. 2004). The three MAPKs, MPK3, MPK4 and MPK6 were also found to be involved in pathogen signaling (Colcombet and Hirt 2008). Recently it has been reported that transgenic tobacco plants ectopically expressing *AhMPK3* exhibited enhanced resistance to *Spodoptera litura* and constitutively expressed defense response genes (Kumar et al. 2009).

Abiotic stress induces the accumulation of ROS in plants, and MAPK signaling pathways are not only induced by ROS but can also regulate ROS production (Pitzschke and Hirt 2009). Overexpressing of *ZmMPK7* in *Nicotiana tabacum* provides protection against ROS-mediated injury by enhancing peroxidase (POD) activity under osmotic stress (Zong et al. 2009). In rice, the MAPKKK DSM1 functions as an early signaling component in response to drought stress by regulating scavenging of ROS (Ning et al. 2010).

Phylogenetic trees reveal that plant MAPKs can be divided into at least four groups (A–D) (MAPK Group 2002). The most extensively studied MAPKs are in groups A and B, and information about plant group C MAPKs is emerging (Doczi et al. 2007; Wang et al. 2007; Zong et al.

2009; Shi et al. 2010; Zhang et al. 2011). However, little is currently known about the function of group D MAPKs. AtMPK18, a group D MAPK, helps to mediate cortical microtubule functions in *Arabidopsis* (Walia et al. 2009). *ZmMPK6* is a unique group D MAPK, found in maize. It is able to interact with 14-3-3 proteins (Lalle et al. 2005). In the monocot model plant rice, several group D MAPKs (OsBWMK1, OsBIMK2 and OsMPK15 etc.) were found to be involved in both biotic and abiotic stress responses (Liu and Xue 2007). Out of the 17 known rice MAPKs, 11 are classified as group D, while only one or two genes fit into groups A–C. The plethora of rice genes and a relatively smaller number of *Arabidopsis* MAPKs in the D group indicate that this group of genes should have some important function in monocot plants (Liu and Xue 2007). Complete sequencing of the maize genome has revealed that maize proteins are more similar to those of rice than to *Arabidopsis* proteins (Alexandrov et al. 2009). In light of the present results, the proposed rice model for monocot plants should fit well for maize—an important cereal crop worldwide.

In this study, we isolated and characterized a novel group D MAPK gene, *ZmMPK17*, from maize. Northern-blot analyses demonstrated that *ZmMPK17* was transcriptionally regulated by multiple stresses. Overexpression of *ZmMPK17* in tobacco is shown to enhance resistance low temperatures and viral infection. In addition, there was less accumulation of ROS than would be expected for plants under similar osmotic stress conditions.

Materials and methods

Plant materials, growth conditions and treatments

Maize seedlings (*Zea mays* L. cv Zhengdan958, from Shandong Agricultural University, China) were grown in Hoagland's solution (pH 6.0) under greenhouse conditions at 22/26°C (night/day), photosynthetic active radiation of 200 $\mu\text{mol m}^{-2} \text{s}^{-1}$, and a photoperiod of 14/10 h (day/night) for 2 weeks.

Tobacco plants (*Nicotiana tabacum* cv NC 89, from Shandong Agricultural University, China) were also used in this study. The transgenic and wild-type tobacco lines were grown for 6 weeks in soil and quartz sand under controlled environmental condition with a photoperiod of 16/8 h (day/night), a temperature of 25/20°C (day/night) and photosynthetic active radiation of 200 $\mu\text{mol m}^{-2} \text{s}^{-1}$.

The 2-week-old maize seedlings were incubated with Hoagland's solution containing 20% PEG6000 (w/v), 100 μM abscisic acid (ABA), 1 mM salicylic acid (SA), 100 μM methyl jasmonates (MeJA), 1 mM ethylene, 1 mM sodium nitroprusside (SNP) or 10 mM hydrogen peroxide (H₂O₂) at 26°C with a continuous light intensity

of $200 \mu\text{mol m}^{-2} \text{s}^{-1}$. Low temperature treatment was carried out at 4°C under the same lighting condition, and plants were watered with Hoagland's solution. To examine the roles of Ca^{2+} and ROS manipulators, the seedlings were pretreated with 2 mM EGTA, 20 mM imidazole, 10 mM Tiron, or 5 mM dimethylthiourea (DMTU) for 12 h and then exposed to 20% PEG6000 (w/v) or 4°C under the same conditions. Samples were collected at the indicated times and all samples were frozen in liquid nitrogen immediately after collection and stored at -80°C . Six-week-old transgenic and the wild-type tobacco lines incubated in quartz sand and soil were treated with 20% PEG6000 or at 4°C under the conditions described above, after which second and third leaf samples were taken.

Cloning of full-length cDNA

Total RNA from untreated maize leaves was extracted with Trizol reagent (Invitrogen) according to the manufacturer's protocol. First strand cDNAs were synthesized using First Strand cDNA Synthesis kit (Fermentas). PCR was performed with gene-specific primers (forward CTGGACATGGACTTCTTCACGGAAT and reverse CTTTTGCCTAACAGGTGACGAGCCT); the products were cloned into pMD18-T vectors (TaKaRa, Beijing, P.R. China) and sequenced. The amino acid sequences of the MAPK proteins of other plants were retrieved from GenBank. Sequence alignments and phylogenetic trees were constructed using DNAMAN 6.0 software.

Northern-blot analysis

Seedlings were treated with different stresses as described above. Total RNA was extracted using the RNeasy plant mini kit (Tiangen, Beijing, P.R.China) according to the manufacturer's instructions and stored at -80°C before being used for northern-blot analysis. 20 μg of total RNA was separated by denaturing 1.0% (w/v) agarose gel, stained with ethidium bromide to ensure equal loading, and then transferred to nylon membranes (Hybond-N+, Amersham Biosciences). A specific fragment of 500 bp at the 3'-end of the *ZmMPK17* cDNA was used as probe. Northern blots were performed as previously described (Zong et al. 2009). The probe was amplified with primers (forward CAAAGGCTGGTGTGAGAGAAATGAT and reverse CTTTTGCCTAACAGGTGACGAGCCT). All experiments were repeated at least two times with identical results.

Subcellular localization of *ZmMPK17*-GFP fusion proteins

The whole coding sequence of *ZmMPK7* was amplified with primers (forward CGTCGACATGGACTTCTTCA

CGGAAT *SalI* site underlined and reverse CGGATCCCAGCCTCGGAGATCCCTTCT *BamHI* site underlined). The kinase domain (KD) of *ZmMPK17* was amplified with primers (forward CGTCGACATGGACTTCTTACGG AAT *SalI* site underlined and reverse CGGATCCA AAGTCAACCTTCAAAATTGG *BamHI* site underlined). The C-terminal domain extension (CD) of *ZmMPK17* was amplified with primers (forward CGTCGACATGGAAT TCGAGGGAAGGAAACTA *SalI* site underlined and reverse CGGATCCCAGCCTCGGAGATCCCTTCT *BamHI* site underlined). These coding sequences were inserted into the reconstructed binary vector pBI121-GFP, which generated a C-terminal fusion with the green fluorescence protein (GFP) gene controlled by the cauliflower mosaic virus (CaMV) 35S promoter. The recombinant plasmids were introduced into *Agrobacterium tumefaciens* strain LBA4404. These plasmids and GFP alone were introduced into onion (*Allium cepa*) epidermal cells by agroinfiltration (Shi et al. 2010). After transformation, tissues were incubated on MS agar medium under dark condition at 23°C for 16 h. Transformed onion cells were observed under a confocal microscope (Olympus, Tokyo, Japan). This experiment was repeated three times at least with identical results.

In vitro mutagenesis of *ZmMPK17*-AF

To produce a kinase-negative version of *ZmMPK17* and *ZmMPK17*-AF, the dual phosphorylation of threonine (T) and tyrosine (Y) residues in the activation loop was mutated to alanine (A) and phenylalanine (F), respectively. *ZmMPK17*-AF was generated using overlap extension PCR as has been described (Heckman and Pease 2007). Two fragments of *ZmMPK17* with overlapping regions were generated using a combination of primers (forward CTA TCTATTGGGCTGATTTTGTGCGCAACAAG and reverse CTTGTTGCGACAAAATCAGCCCAATAGATAG) in the first round of PCR. Full-length mutated *ZmMPK17* was obtained by combining the two products obtained in first round of PCR and using these as template for the second round with gene-specific primers. The product was designated as *ZmMPK17*-AF and cloned into pMD18-T. The presence of the desired mutation was confirmed by sequencing.

Overexpression of *ZmMPK17* and *ZmMPK17*-AF in tobacco

The full correct coding regions of *ZmMPK17* and *ZmMPK17*-AF ligated into the binary pBI121 expression vector under the control of the CaMV 35S promoter. Transformation of tobacco was performed as has been described (Zong et al. 2009).

Histochemical detection of H₂O₂ and O₂⁻

H₂O₂ accumulation was detected by the 3,3'-diaminobenzidine (DAB) and O₂⁻ using nitroblue tetrazolium (NBT) staining methods. The seedlings infiltrated with 5 mg/ml DAB at pH 3.8 for 20 h and 0.5 mg/ml NBT for 20 h in the dark to detect H₂O₂ and O₂⁻ respectively. Then the seedlings were decolorized by boiling in ethanol (96%) for 10 min. After cooling, the leaves were extracted at room temperature with fresh ethanol and photographed using a stereomicroscope. Each experiment was repeated three times at least with identical results.

Measurements of physiologic parameters

Tobacco seedlings were treated with 20% PEG 6000 for indicated time, and then 0.5 g of leaves was collected for catalase (CAT) and APX measurements that were performed as described previously (Zhang et al. 2011). In addition, 0.5 g of leaves was collected for H₂O₂ measurements, which were performed as described by Jiang and Zhang (2001). Relative electrolytic leakage was determined following the methods of Liu et al. (2009).

The 14-day-old seedlings of transgenic and control were treated with methyl-viologen (MV) for the indicated lengths of time. Chlorophyll was extracted using 95% ethanol and analyzed using UV spectrophotometry (Zhang et al. 2011).

Tobacco seedlings were kept at 4°C for the indicated lengths of time. Then 0.5 g of leaves was collected for measurement of soluble sugars and proline. These were performed as has been described previously (Irigoyen et al. 1992).

Germination experiments

About 50 surface-sterilized seeds from each homozygous T2 transgenic lines and wild-type tobacco lines were plated on solid media composed of MS basal salts and 0.8% sucrose. To determine cold-stress sensitivity, plates were incubated in a controlled-environment growth chamber at 8°C with a photoperiod of 16/8 h (day/night). Twenty-six days latter, the rates of seed germination were evaluated (root emergence). Each experiment was repeated three times at least with identical results.

Semi-quantitative RT-PCR

Extraction of total RNAs and reverse transcription were performed as described above. PCR amplifications were carried out in a thermo-cycler and programmed for pre-denaturation at 95°C for 5 min, followed by 28 cycles at 95°C for 1 min, 56°C for 50 s and 72°C for 45 s, and the final

extension at 72°C for 10 min. Amplified genes and their respective primers are listed below. The *NtACTIN* gene was amplified in the same cDNA pool as the internal control to monitor the PCR efficiency. *NtACTIN* (X69885): forward CTATTCTCCGCTTTGGACTTGGCA and reverse ACC TGCTGGAAGGTGCTGAGGGAA; *NtAPX* (U15933): forward TCCCACTGTAAGCGAGGAGT and reverse CA GATAGACCCATTTGCTTCAC; *NtCAT1* (NTU93244): forward GTACCGTCCGTCAAGTGCCT and reverse GCAGGCTTTCAGGAACATGAG; *NERD10B* (AB049336): forward TATGGGAACCCAGTCCATCACACTGGA and reverse CTTTAAAGGGATTTTATTGTTTGGCAG; *NtERD10C* (AB049337): forward AGGTTGAAGAGGGTAC CGAAACG and reverse GCCACTTCCTCTGTCTTCT TTTGC; *PR1a* (X12485): forward GATGCCATAACA CAGCTCG and reverse GATCATACATCAAGCTGATC; *PR5* (AF154636): forward ATGCTTCTGACTTTGGAT GAG and reverse CCAGGTCATCTGATTCAATC; *PR4* (EH365959): forward GAGCATGATGGTGGCAATGGC and reverse TCATAGTTGACAATAAGGTGGC; *EREBP* (CN748856): forward GAATTGCACTGCACTTGATTTG and reverse GCCTTAGCCGCCTGTATGGC. All primers were designed using PRIMER 5.0 to avoid detecting other homologous sequences. RT-PCR reactions were repeated four times at least with identical results.

Pathogen infection and enzyme-linked immunosorbent assay (ELISA) detection

Virus infection and ELISA detection were performed according to methods developed by Zhang et al. (2011). Briefly, 4-week-old tobacco plants were inoculated with 100 µl of a CMV and PVY suspension inoculum (CMV and PVY in 50 mM phosphate buffer, pH 7.2) by rubbing the fully expanded second and third true leaves with wet carborundum followed immediately by rinsing with deionized water. Tobacco plants inoculated with 100 µl of buffer were used as controls. Virus accumulation was determined by ELISA. Purified CMV and PVY were used to prepare polyclonal antisera. A 1:4,000 (v/v) dilution of HRP-conjugated goat anti-rat IgG (Zhongshan, Beijing, P.R.China) was used to detect anti-CMV and anti-PVY antibodies. Optical density was measured at 492 nm with an ELISA plate reader. The upper uninoculated seventh true leaves were harvested 15 days after inoculation for CMV detection. Sixth true leaves were harvested 30 days after inoculation for PVY detection. Each experiment was repeated three times at least with identical results.

Statistical analysis

Statistical analyses were performed using SigmaPlot11.0 and SPSS13.0 software. Mean values ± SD of at least

three replicates are presented, and significant differences relative to controls are given at $P < 0.01$ and $P < 0.05$.

Results

Cloning and characterization of *ZmMPK17*

In order to isolate genes involved in the early steps of maize plant defense/stress response pathways, we use specific primers to isolate fragment of the MAPK gene from maize. This gene is highly similar to *AtMPK17* (GenBank accession number: NM001035683, 65% identity), so we designate this fragment *ZmMPK17* (GenBank accession number: JF422063) according to the existing nomenclature of plant MAPKs (MAPK Group 2002).

The *ZmMPK17* gene has an open reading frame of 1,476 bp encoding a protein of 491 amino acid residues with an estimated molecular mass of 55.6 kD. Alignment of the deduced protein sequence with other MAPKs from plants indicated that *ZmMPK17* contains all 11 conserved subdomains that are characteristic of serine/threonine protein kinases. A specific dual phosphorylation activation motif TDY (aa 175–177) was found, along with a P loop, C loop, and activation loop (between subdomains VII and VIII) (Fig. 1a). In addition to the conserved protein kinase domains, *ZmMPK17*, along with its homolog in rice, *OsBIMK2* (AY524973, 74.8% identity), *OsBWMK1* (AF117392, 69.74% identity), and *OsMPK15* (ABA92669, 63% identity) and *Arabidopsis AtMPK17* has a C-terminal region extension, which is not seen in other plant MAPKs. This C-terminal region shows a high level of variation (Fig. 1a). Based on the amino acid sequences of *ZmMPK17* and other plant MAPKs, phylogenetic tree analysis showed that *ZmMPK17* belongs to group D (Fig. 1b).

It is convenient to analyze the genomic structure of *ZmMPK17* as the final completion of the *Zea mays* genome sequencing. Alignment of *ZmMPK17* with maize genomic sequences (<http://www.plantgdb.org/ZmGDB>) revealed that the *ZmMPK17* gene is located on chromosome 4 and the coding region contains ten exons and nine introns (Fig. 1c). All introns showed a high AT content, in particular they had an elevated T content, which is a peculiar feature of many plant introns (Ko et al. 1998).

The C-terminal domain extension (CD) of *ZmMPK17* is essential for its nuclear localization

MAPKs can phosphorylate target proteins in both the cytoplasm and nucleus. Evidence shows that a correlation exists between the subcellular localization of MAPK and the resulting cellular responses (Mutalik and Venkatesh 2006). To determine the subcellular localization of MAPK

in vivo, full-length, *ZmMPK17* kinase domain (KD) and CD was fused in frame to the N-terminus of the GFP reporter gene under the control of the CaMV 35S promoter (Fig. 2a). These constructs and GFP alone were introduced into onion (*Allium cepa*) epidermal cells by agroinfiltration. As shown in Fig. 2b, the *ZmMPK17*-GFP and CD-GFP fusion protein specifically accumulated in the nucleus, whereas KD-GFP and GFP alone were present throughout the whole cell. Thus, it can be concluded that the CD of *ZmMPK17* is essential for its targeting to the nucleus.

Differential effects of diverse environmental cues on the expression of *ZmMPK17*

To assess the expression patterns of *ZmMPK17*, we performed northern-blot analysis. First, we investigated its expression in different tissues. As shown in Fig. 3a, *ZmMPK17* was ubiquitously detected in roots, stems and leaves. The transcription level in the roots was higher than that in the stems and leaves. Its expression level in the stem was minimal. These results indicated that *ZmMPK17* was expressed in different tissues at different levels. Treatment of PEG (20%) resulted in a decline in *ZmMPK17* expression, whereas low temperature (4°C) led to an increase in *ZmMPK17* expression after 3 h of treatment. The treatment effects became more and more prominent with time (Fig. 3b, c). ABA is an important phytohormone, mediating some aspects of the physiological response to environmental stress (Zhu 2002). Administration of 100 μM ABA to the seedling resulted in no significant increase in transcription of *ZmMPK17* within less than 12 h of treatment, however, a significant increase was observed by 24 h (Fig. 3d).

The phylogenetic tree of *ZmMPK17* shows that *ZmMPK17* is evolutionarily related to *OsBIMK2*, *OsBWMK1* and *OsMPK15*, which are implicated in response to various biotic stresses (Reyna and Yang 2006). These results lead us to further examine the response of *ZmMPK17* to SA, JA and ethylene, which are known to play major roles in regulating plant defense responses against various pathogens and pests (Bari and Jones 2009). After treatment with 1 mM SA, transcription levels of *ZmMPK17* increased rapidly for 1 h and then declined. Another peak emerged at 6 h (Fig. 3e). It was also found that the response of *ZmMPK17* to 100 μM MeJA began at 1 h after treatment and was alleviated at 6 h, but this upregulation reappeared at 12 h (Fig. 3f). This pattern was similar to that of GhMAPK from cotton (*Gossypium hirsutum* L.) under salt stress (Wang et al. 2007). This also suggests the existence of a feedback adjustment. *ZmMPK17* transcription increased after ethylene treatment and reached a peak at 24 h (Fig. 3g).

Nitric oxide (NO) has attracted attention as a radical that participates in various physiological processes in plants.

Recent evidence indicates that NO activates the MAPK cascade and increases the expression of defense genes (Yoshioka et al. 2010). To determine whether *ZmMPK17* expression was triggered by NO, maize seedlings were exposed to 1 mM SNP, an NO donor. However, *ZmMPK17* showed a negligible response to SNP treatment (Fig. 3h). There was no change in *ZmMPK17* transcription level in the roots and leaves under normal condition during 0–24 h observation series (Fig. 3i, j).

Mediation of osmotic stress and low temperature-induced expression of *ZmMPK17* by H₂O₂ and Ca²⁺

As shown in Fig. 3a, b, the transcription level of *ZmMPK17* in the roots was higher than that in the leaves, and the level of transcription in the leaves gradually declined under osmotic stress. Under osmotic stress conditions, the roots dried out before the leaves did, suggesting that the extent of downregulation in the roots would be more severe than in the leaves. These results lead us to further examine the response of *ZmMPK17* to osmotic stress in the root tissue. PEG (20%) treatment resulted in a decreased level of *ZmMPK17* mRNA in the roots (Fig. 3k). Furthermore, 10 mM H₂O₂ caused a marked decrease in transcription level at 3 h in roots, followed by a gradual recovery to an untreated level (Fig. 3l).

Both PEG and H₂O₂ treatment caused a decline in the expression of *ZmMPK17*, and the lower peaks appeared at 24 and 3 h, respectively (Fig. 3k, l). To examine whether H₂O₂ mediated PEG-induced *ZmMPK17* transcription, seedlings were pretreated with several ROS manipulators, including imidazole, an inhibitor of reduced nicotinamide adenine dinucleotide phosphate (NADPH) oxidase, and the H₂O₂ scavengers Tiron and DMTU (Zong et al. 2009). Pretreatment with these ROS inhibitors and scavengers partly alleviated the PEG-induced downregulation of *ZmMPK17* transcription (Fig. 3m), especially at 24 h, indicating that H₂O₂ is required for PEG-induced decreases in *ZmMPK17* mRNA.

Ca²⁺ is an important second messenger in plant cells, and a change in its cytosolic concentration is a component of the signaling network that is triggered in response to environmental stimuli. EGTA, which chelates extracellular Ca²⁺, was used to determine whether Ca²⁺ takes part in the effects of low temperature and osmotic stress on *ZmMPK17* transcription. Pretreatment of seedlings with EGTA arrested the low temperature and PEG-induced upregulation and downregulation of *ZmMPK17* mRNA (Fig. 3m, n), suggesting that increased Ca²⁺ in the cytoplasm may act as a second messenger causing changes in *ZmMPK17* expression.

Fig. 1 Alignment, phylogenetic relationships and properties of *ZmMPK17*. **a** Alignment of *ZmMPK17* with MAPKs from other plant species: OsBIMK2 (AY524973), OsMPK15 (ABA92667), OsBWMK1 (AAD52659), and AtMPK17 (NM001035863). Protein kinase subdomains are shown with numerals (I–XI) on top. P-loop, C-loop, and activation-loop motifs are boxed, and the conserved motif TDY is indicated by asterisks. **b** Phylogenetic tree of *ZmMPK17*. This phylogenetic tree based on the genetic distance of the protein was constructed by the Clustal method using DNAMAN 6.0 software. The plant MAPK proteins used for alignment are *Arabidopsis thaliana* AtMPK1 (NP172492), AtMPK3 (BAA04866), AtMPK4 (BAA04867), AtMPK6 (BAA04869), AtMPK7 (NP179409), AtMPK15 (NM106026), AtMPK17 and AtMPK18 (NM104229); *Oryza sativa* OsBWMK1, OsBIMK2, OsMPK15, OsMSRMK3 (CAD54741) and OsWJUMK1 (CAD54742); *Nicotiana tabacum* NtNTF3 (CAA49592), NtNTF6 (CAA58760), NtSIPK (AAB58396) and NtWIPK (BAA09600); and *Zea mays* ZmMPK5 (BAA74734) and ZmMPK4 (AB016801), ZmMPK6 (AY425817), ZmSIMK (DQ422149), ZmMPK7 (ABC02871), and ZmMPK17. **c** Schematic representation of *ZmMPK17* structure. Exons are represented by boxes and introns by lines. The lengths of individual exons and introns are given in base pairs. ATG and TGA are indicated by arrows. Drawings are not exactly to scale

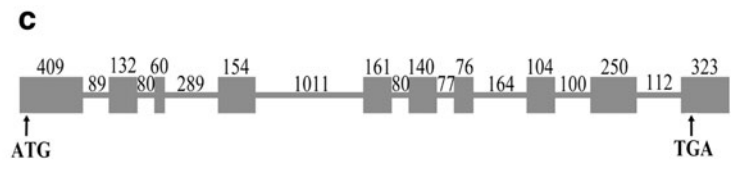
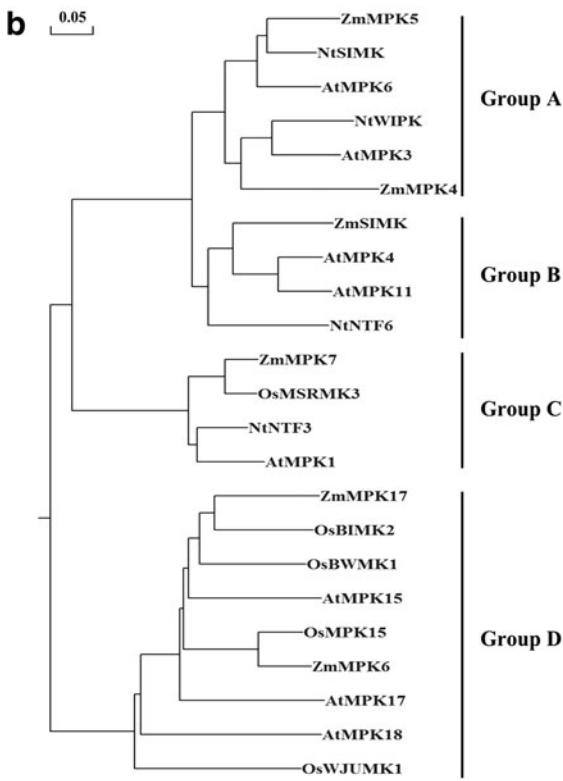
Overexpressing *ZmMPK17* in *Nicotiana tabacum* enhanced ability of ROS scavenging under osmotic stress

In order to obtain more information on the biological function of *ZmMPK17* in plants, *ZmMPK17* and *ZmMPK17-AF* were overexpressed in tobacco under the control of the CaMV 35S promoter. Independent transgenic lines were obtained by kanamycin-resistance selection and confirmed by genomic PCR (data not shown). Northern-blot analysis revealed that *ZmMPK17* and *ZmMPK17-AF* were expressed normally in engineered lines (Fig. 4a, b), but no expression was detected in the wild-type plants, as expected. T2 transgenic plants from six representative lines (OE-25, OE-24, OE-11, AF-22, AF-11, and AF-9) were selected for further experimentation.

Abiotic stress results in the accumulation of ROS in plants. For this reason, we evaluated the accumulation of H₂O₂ and superoxide radical anions (O₂⁻) in transgenic seedlings under osmotic stress. Homozygous T2 transgenic tobacco and wild-type seeds were germinated on MS medium plates for 2 weeks and then transferred to MS plates supplemented with 400 mM mannitol, which mimics osmotic stress. After 2 weeks of treatment, WT and *ZmMPK17-AF*-overexpressing (AF) plants showed a greater accumulation of H₂O₂ and O₂⁻ than *ZmMPK17*-overexpressing (OE) lines in the shoot apex, cotyledon and root, as indicated by the accumulation of brown (DAB staining) and blue (NBT staining) pigments (Fig. 5a). Under normal growth conditions, no obvious H₂O₂ or O₂⁻ were detected in either wild-type or transgenic seedlings (data not shown). Furthermore, H₂O₂ was also detected in

a

	Subdomain I	P-loop	Subdomain II	Subdomain III	Subdomain IV		
ZmMPK17	...MDF	FTEYGEASQYCIQEV	IGKGSYGVVA	AAIDSH	TGERLAIKKINDI	GNVSDAARILREIKLRLRLRHENIVQIKHIMLPETTRREFKDIYVVFELM 97	
OsBIMK2	...MEF	FTEYGEASQYCIQEV	VGKGSYGVVA	AAVDTHT	GERVAIKKINDV	FEHVSDAIRILREIKVLRLLRHEDIIVIKHIMLPETTRREFKDIYVVFELM 97	
OsBWMK1	...MEF	FTEYGEASQYCIQEV	IGKGSYGVVA	AAVDTHT	GERVAIKKINDV	FEHVSDAIRILREIKLRLRLRHEDIIVIKHIMLPESRREFKDIYVVFELM 97	
OsMPK15	...MDF	FTEYGEASQYCIQEV	IGKGSYGVVCS	ALDTH	TGEKVAIKKINDI	FEHVSDAIRILREIKLRLRLRHEDIIVIKHIMLPESRREFKDIYVVFELM 97	
AtMPK17	MLEKE	FTEYGEASQYCIQEV	VGKGSYGVVA	SAECPH	IGKVAIKKMTNV	FEHVSDAIRILREIKLRLRLRHEDIIVIKHIMLPETTRREFKDIYVVFELM 100	
Subdomain V							
	Subdomain V	C-loop	Subdomain VII	Activation-loop	Subdomain VIII		
ZmMPK17	ESDLHQV	IKANDNITPEHHR	FFLYQLIRAL	KYMHS	AVFHRDLKPKNILANS	SDSKLKICDFGLARASFNISLSAIYWTIDYVATRWRAPELCGSFFSSYT 197	
OsBIMK2	ESDLHQV	IEANHDLSEHHR	FFLYQLCAL	KYIHS	NVFRDLKPKNILANS	SDCKLKICDFGLARVAFNISPSSTIFWTDYVATRWRAPELCGSFFSKYT 197	
OsBWMK1	ESDLHQV	IRANDDITPEHYQ	FFLYQLIRAL	KYIHS	NVFRDLKPKNILANS	SDCKLKICDFGLARASFNISPSAIWTDYVATRWRAPELCGSFFSKYT 197	
OsMPK15	ESDLHQV	IKANDDITPEHYQ	FFLYQLRGL	KYIHS	NVFRDLKPKNILANS	SDCKLKICDFGLARVAFNISPTAIFWTDYVATRWRAPELCGSFFSKYT 197	
AtMPK17	ESDLH	VLVKNDITPEHHR	FFLYQLRGL	KFMHS	AVFHRDLKPKNILANS	SDCKLKICDFGLARVFNISPSAVFWDYVATRWRAPELCGSFFSNYT 200	
Subdomain IX							
	Subdomain IX	Subdomain X	Subdomain XI				
ZmMPK17	PAIDIN	SIGCIFAELTG	RPLPFG	RNVVHQ	LDLIT	DLLGTPSFRSLSCVHSDKAREYLLGMFRKRPIFESHKFNADPLALRLERLLAFDKDRPTAEE 297	
OsBIMK2	PAIDIN	SIGCIFAELTG	RPLPFG	RNVVHQ	LDLIT	DLLGTPSFRSLSRIRNENARGYLTMQRKHPPIFESHKFNADPLALRLERLLAFDKDRPTAEE 297	
OsBWMK1	PAIDIN	SIGCIFAELTG	RPLPFG	RNVVHQ	LDLIT	DLLGTPSFRSLSRIRNEKARRYLSNRKKHVPFSCFRNTEPLALRLERLLAFDKDRPTAEE 297	
OsMPK15	PAIDIN	SIGCIFAELTG	RPLPFG	RNVVHQ	LDLIT	DLLGTPSTEATSRIRNEKARRYLSNRKRKPIFESHKFNADPLALRLERLLAFDKDRPTAEE 297	
AtMPK17	PAIDIN	SIGCIFAELTG	RPLPFG	RNVVHQ	LDLIT	DLLGTPSPITLSRIRNEKARKYLGNNRRKDPVFFTHKFNIDPVALRLERLLAFDKDRPTAEE 300	
ZmMPK17	ALADPY	FRGISKLS	REPSR	LVSK	FEFERR	KLTKDDVRELIYREILEYHQMLQCYEYIRGGEQIS..FLYPSGVDRFKRQFAHLEENYSRGERSTPL.. 393	
OsBIMK2	ALADPY	FRGISKLS	REPSR	LVSK	FEFERR	KLTKDDVRELIYREILEYHQMLQCYEYIRGGEQIS..FLYPSGVDRFKRQFAHLEENYSRGERSTPL.. 393	
OsBWMK1	ALADPY	FRGISKLS	REPSR	LVSK	FEFERR	KLTKDDVRELIYREILEYHQMLQCYEYIRGGEQIS..FLYPSGVDRFKRQFAHLEENYSRGERSTPL.. 393	
OsMPK15	ALADPY	FRNISAN	VDRPS	AVTK	LEFEFERR	ITKEDIRELIYRILEYHQMLQCYEYIRGGEQIS..FLYPSGVDRFKRQFAHLEENYSRGERSTPL.. 397	
AtMPK17	ALADPY	QGLAN	VDRPS	RQV	ISLLEFEFERR	KLTKDDVRELIYREILEYHQMLQCYEYIRGGEQIS..FLYPSGVDRFKRQFAHLEENYSRGERSTPL.. 400	
ZmMPK17	RRQPT	SLPRERVCS	SEDGHS	QSDS	EEQRAASYVARTIISFPRSQEEGGKLQPAYQSAADSCAKSYLKGAAISSASRRITKGDNG 482	
OsBIMK2	RRQPT	SLPRERVCS	SVDSN	NQSD	NEERRAIISSARTMISFPRSQEEGGKLRASAYPNGLINLNSPKIYLS.ASI.SASTCIIRG.NK 479	
OsBWMK1	RRQPT	SLPRERVCS	SKDGN	YQNT	NDQERSADSVARTIVSPPMSQDAQHG.SAGQNGVTSTDLSSRSYLS.ASI.SASKVAVKDNK 479	
OsMPK15	NSLPR	PSVLYS	DRPQNT	ANIAEDL	SKCVL	GDNTQKMHQGSASVCANRPVQGGAAARPGKVVGSALRYGNCSTSTAEQYHRRTRDRNPALATNTVSPRGSY 497	
AtMPK17	RRQPT	SLPRERVCS	SEDEGS	D	SVAHQSS.SASVVTFPPQENTATGLSSQKASQVDKAATPVKRSACLMSRSDSICASRCVGVSSAV 485	
ZmMPK17	RKEK	GS	SPRL				491
OsBIMK2	GPKEN	GIS	EDM	EEV	VEL	SDNV	TRML 505
OsBWMK1	EPEDDY	I	SE	ME	GS	V	DGLSEQVSRMH 505
OsMPK15							498
AtMPK17							



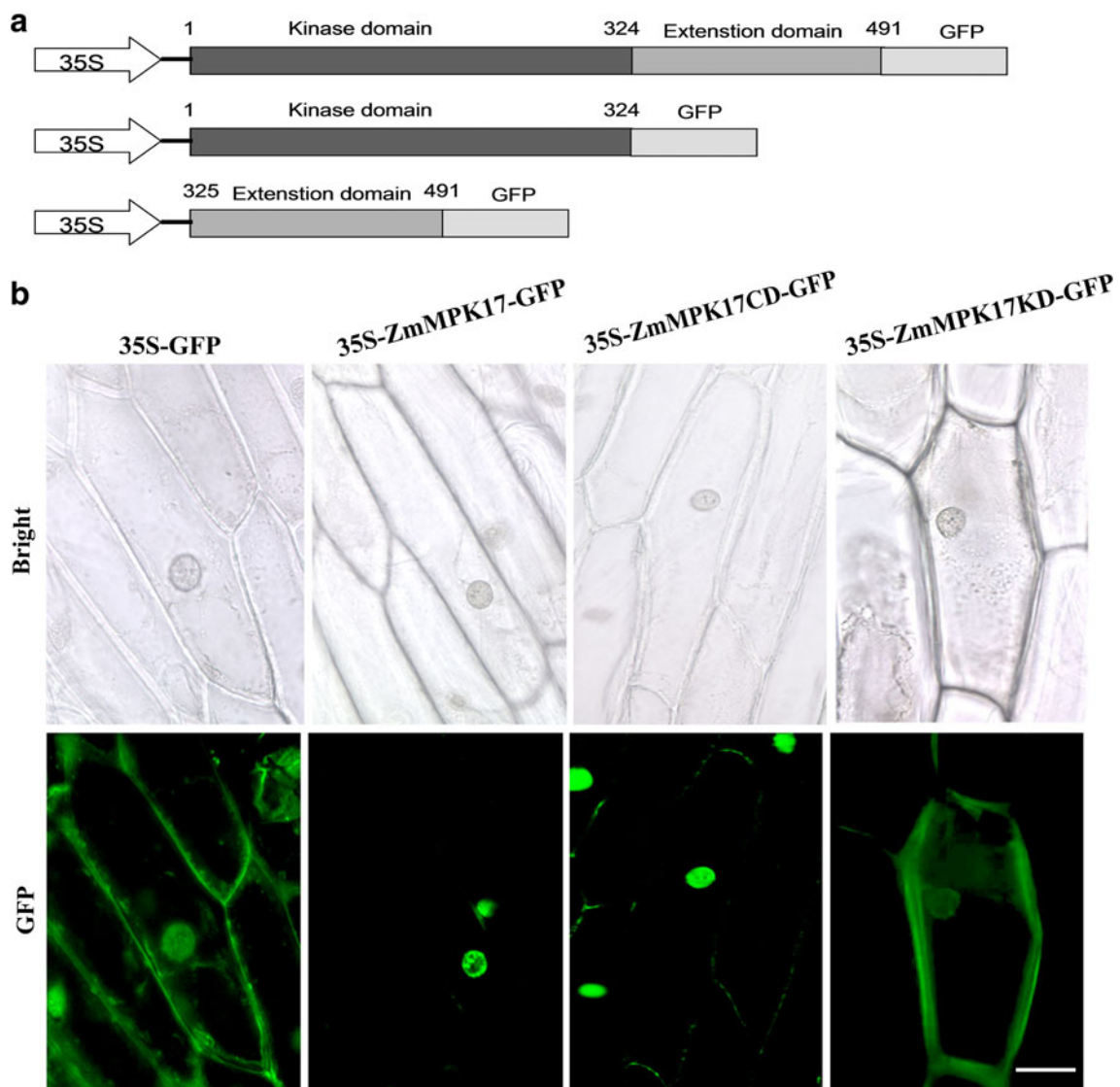


Fig. 2 Subcellular localization of ZmMPK17. **a** Schematic diagram of GFP fusion constructs of ZmMPK17. Amino acid numbers of domains and boundaries are indicated. **b** Transient expression of 35S-GFP, 35S-ZmMPK17-GFP, 35S-ZmMPK17CD-GFP and 35S-

ZmMPK17KD-GFP in onion epidermal cells was via agroinfiltration. GFP was visualized in epidermal cells by confocal laser scanning microscopy 16 h post-agroinfiltration. This experiment was repeated at least three times with identical results. Bar 50 μ m

the 6-week-old plants after 20% PEG treatment, H_2O_2 content increased in all lines after PEG treatment. However, relative to WT and AF lines, OE lines accumulated a much lower level of H_2O_2 under osmotic stress conditions (Fig. 5b). These results suggested that overexpression of *ZmMPK17* in tobacco could effectively alleviate the accumulation of ROS.

Previous studies have shown that overexpression of *ZmMPK7* in transgenic tobacco resulted in enhanced peroxidase (POD) activity to protect the plant from ROS-mediated injury (Zong et al. 2009). To determine whether *ZmMPK17* upregulates the activities of antioxidant enzymes, antioxidant enzyme activity in soluble protein extracts taken from the osmotically stressed leaves of

transgenic and WT plants were measured. Ascorbate peroxidase (APX) activity was increased after the onset of osmotic stress in both transgenic and WT plants. However, significantly lower APX activity was detected in the WT and AF plants than in the OE lines (Fig. 5c). In contrary, catalase (CAT) activity was decreased after treatment, but the activity in the OE lines was much higher than that in other lines (Fig. 5d). We also analyzed the expression of oxidative stress-related genes including *NtAPX* and *NtCAT1* under osmotic stress conditions. The transcription levels of *NtAPX* showed no marked influence in the control (WT and AF) plants after PEG (20%) treatment. However, in the OE plants, transcription reached a high level at 12 and 24 h, returning to background levels at 48 h. In treated

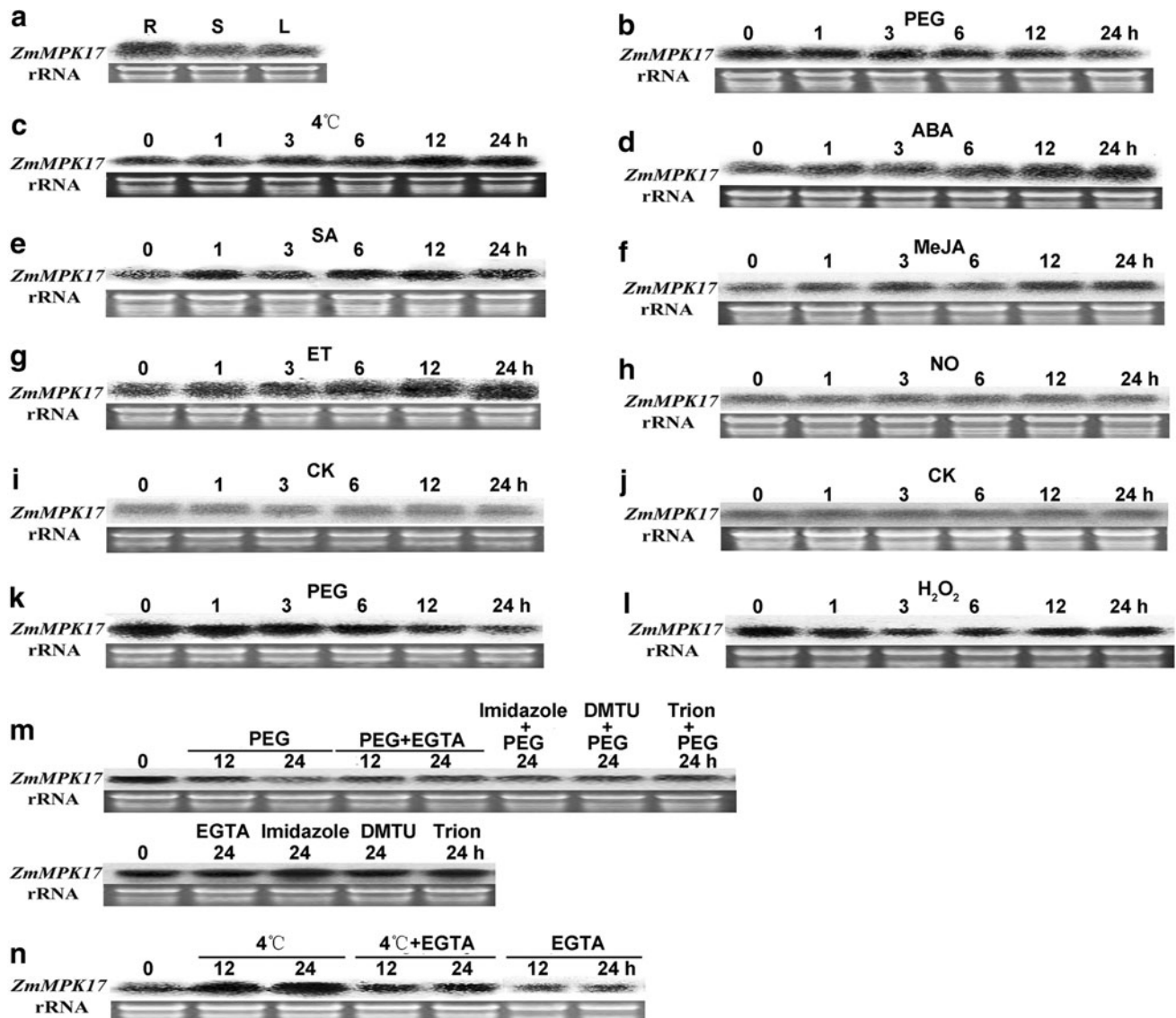


Fig. 3 Northern-blot analysis of the expression of *ZmMPK17*. **a** Tissue-specific expression of *ZmMPK17*. Total RNA was isolated from leaves (L), stems (S) and roots (R), respectively. **b–i, n** Total RNA was isolated from leaves at indicated times; **j–m** Total RNA was isolated from roots at indicated times. Maize seedlings were treated with 20% PEG6000 (w/v), low temperature (4°C), 100 μM ABA, 1 mM SA, 100 μM MeJA, 1 mM ethylene, 1 mM sodium nitroprusside (SNP), 10 mM H₂O₂ or Hoagland’s solution (CK). **m** Maize seedlings were pretreated with 5 mM DMTU, 20 mM

imidazole, 10 mM Tiron or 2 mM EGTA for 12 h, and then treated with 20% PEG6000 for the indicated length of time. Control seedlings were treated with 5 mM DMTU, 20 mM imidazole, 10 mM Tiron or 2 mM EGTA for 24 h. **n** Maize seedlings were pretreated with 2 mM EGTA for 12 h, and then treated with 4°C for the indicated length of time. Control maize was treated with 2 mM EGTA alone. Ethidium bromide stained ribosomal RNA (rRNA) is included as loading control. All experiments were repeated at least two times with identical results

NtCAT1, transcription levels were increased at 12 and 24 h and then suppressed at 48 h in all plants measured, but before treatment, the OE plants presented a higher level than did the other plants (Fig. 5f).

To investigate the effect of *ZmMPK17* overexpression on the physiological response to osmotic stress in tobacco, relative electrolyte leakage was measured since it is the indicator of membrane damage. Relative electrolyte leakage increased in all lines after PEG (20%) treatment; however, the increases were more pronounced in the WT

and AF lines (Fig. 5e). These results indicated that membrane damage caused by osmotic stress was relatively moderate in the OE plants.

To further confirm the ability of *ZmMPK17*-overexpressing tobacco plants to scavenge ROS, the oxidative agent methyl-viologen (MV) was used. As shown in Fig. 5g, the cotyledon bleaching or chlorosis in the WT and AF plants was more severe in media containing 5 μM of MV than in the OE plants. This result was confirmed by measuring chlorophyll content after MV treatment, the OE

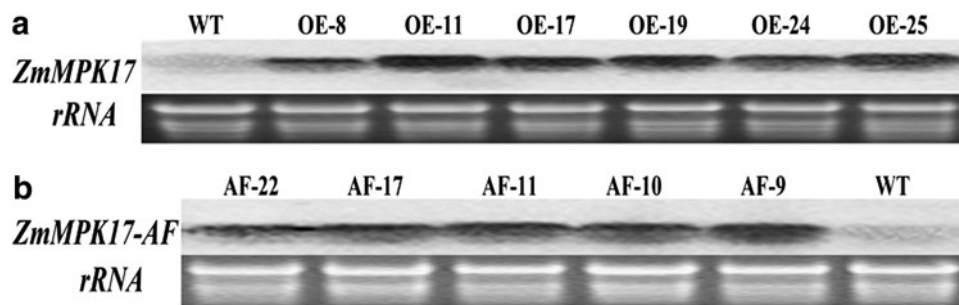


Fig. 4 Northern-blot analysis of *ZmMPK17* and *ZmMPK17-AF*. **a** Transgenic *ZmMPK17*-overexpressing plants (OE). **b** *ZmMPK17-AF*-overexpressing plants (AF). Total RNA was isolated from leaf

samples collected from T2 tobacco plants grown under normal conditions. All experiments were repeated at least two times with identical results

lines showed a higher chlorophyll content than the WT and AF lines (Fig. 5h), suggesting that overexpression of *ZmMPK17* in tobacco confers increased tolerance to oxidative stress.

Together, these observations demonstrate that overexpression of *ZmMPK17* in transgenic tobacco results in ROS scavenging by upregulating the activities of antioxidant enzymes and the expression of oxidative stress-related genes under osmotic stress conditions. In addition, the kinase activity of *ZmMPK17* was essential for full function in plants.

Overexpression of *ZmMPK17* improves tolerance to low temperature stress

Because *ZmMPK17* was inducible by ABA and cold stress (Fig. 3c, d), we examined the effect of *ZmMPK17* overexpression on the tolerance of transgenic plants to cold. Stress tolerance was evaluated based on the germination rate of seeds at low temperatures. Under normal growth conditions, no obvious difference in germination rate was detected in either wild-type or transgenic seedlings (data not shown). The six transgenic lines, including the three OE lines and three AF lines, exhibited significantly increased tolerance to cold stress (Fig. 6a, b).

Accumulation of soluble sugars had been found not only to lower the solute potential in plant cells, but also to sense and control ROS balance. Higher proline concentrations can also protect cell metabolism by avoiding protein denaturation and/or by controlling cell pH (Irigoyen et al. 1992; Couee et al. 2006). Concentrations of soluble sugars and proline in transgenic tobacco and WT plants were analyzed. Before and after treatment at 4°C, concentrations of soluble sugars and proline in transgenic plants were significantly higher than those in the WT plants (Fig. 6c, d). Thus, enhanced cold-insensitive phenotype in the transgenic plants observed in the germination assay manifests itself as cold resistance with respect to the accumulation of free proline and soluble sugars. These results indicate that

ZmMPK17 overexpression increased transgenic tobacco tolerance to cold stress, revealing the function of *ZmMPK17* protein in plants.

Enhanced transcription of *NtERD10* genes in *ZmMPK17*-overexpression lines under osmotic stress and cold stress

To better understand how *ZmMPK17* increase resistance to osmotic and low temperature stress, we examined the expression of *NtERD10*, a family of genes encoding group 2 LEA proteins (Kasuga et al. 2004). Under normal and osmotic stress conditions, overexpression of *ZmMPK17* induced the expression of *NtERD10B* and *NtERD10C*, but the transcription levels were higher in the OE plants, especially at 48 h (Fig. 5f). *NtERD10B* and *NtERD10C* transcription was almost undetectable in the absence of cold stress in the WT and AF plants, but in the OE plants it was greatly elevated even under normal growth conditions (Fig. 6e). These results indicate that these two *NtERD10* genes are target stress-inducible genes of *ZmMPK17* in transgenic tobacco and contribute to the enhanced stress tolerance.

Viral resistance of *ZmMPK17*-overexpression in tobacco plants

To examine the biological functions of the *ZmMPK17* gene in plant defense responses, we inoculated 4-week-old transgenic and WT plants with cucumber mosaic virus (CMV) and potato virus Y (PVY). Fifteen days later, inoculated WT and AF lines showed severe disease symptoms including stuntedness, curled leaves, and other abnormalities. However, only slight disease symptoms were observed in the OE plants (Fig. 7a). ELISA detection revealed that accumulation of CMV in the OE plants was suppressed (Fig. 7b). All three OE lines also showed increased resistance to PVY infection, as indicated by significantly reduced disease severity (Fig. 7c) and PVY

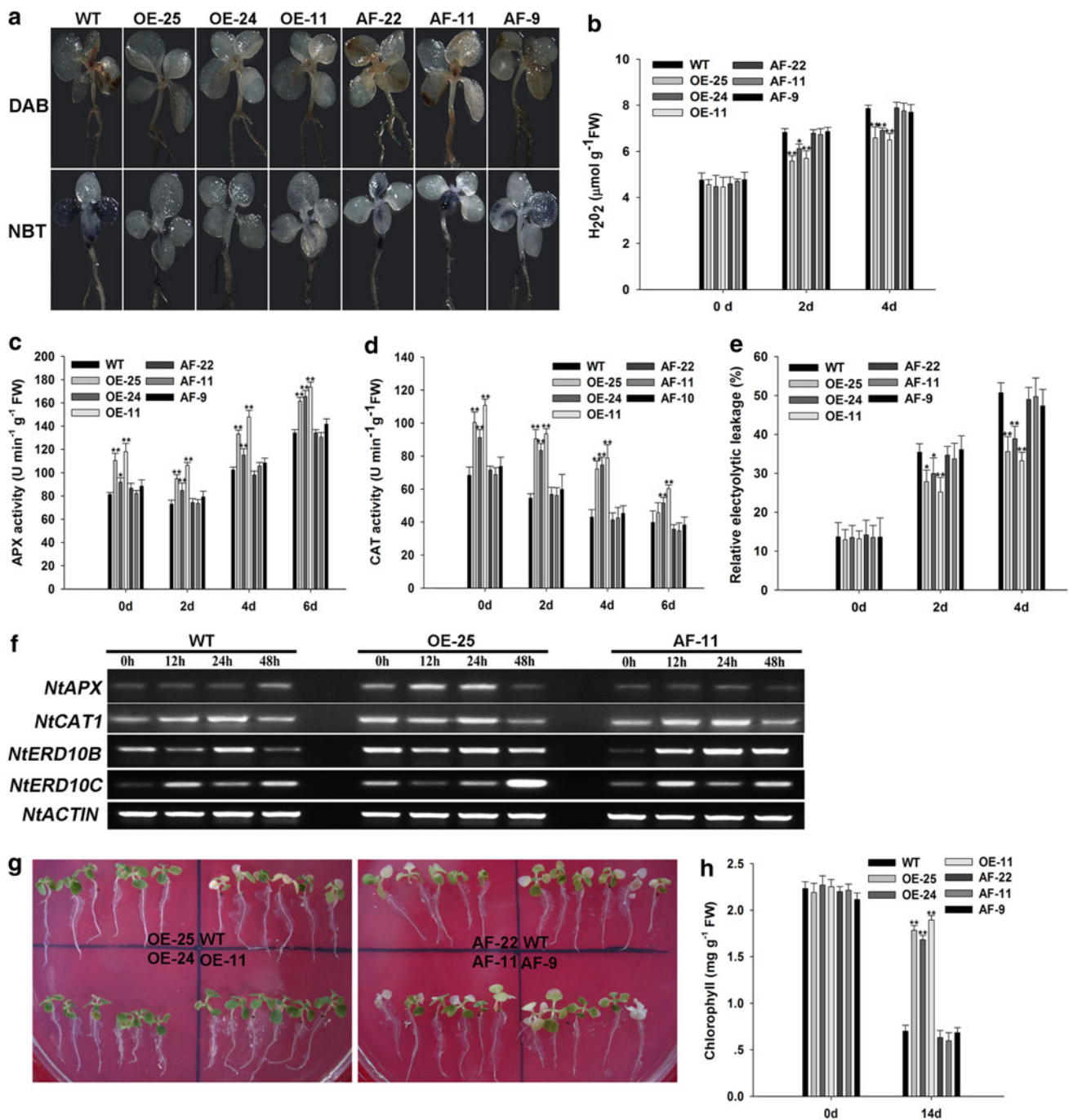


Fig. 5 ROS accumulation, activity of antioxidant enzymes, and expression of stress-related genes in wild-type (WT) and transgenic tobacco under osmotic stress conditions. **a** In situ detection of H₂O₂ and O₂⁻ by DAB (upper) and NBT (lower) staining of WT and transgenic seedlings. Tobacco seeds were germinated on MS medium under normal conditions for 2 weeks and then transferred to MS medium supplemented with 400 mM mannitol for 2 weeks. Images were taken under a stereomicroscope. Each experiment was repeated at least three times with identical results. **b–e** Six-week-old wild-type and transgenic tobacco lines incubated in sand were treated with 20% PEG6000 (w/v) for the indicated lengths of time. The second and third leaves were collected from each plant. The H₂O₂ content (**b**), total activity of the antioxidant enzymes APX (**c**) and CAT (**d**), and relative electrolytic leakage (**e**) were measured. **f** Expression of stress-related genes by

semi-quantitative RT-PCR. Total RNA was extracted from leaf samples at the indicated times after 20% PEG6000 (w/v) treatment. All RT-PCR reactions were from the same batch of cDNA and were repeated at least four times with identical results. **g** Overexpression of *ZmMPK17* confers increased tolerance to oxidative stress. Tobacco seeds were germinated on MS medium under normal conditions for 2 weeks, and then transferred to MS medium supplemented with 5 μM MV for 2 weeks, and then photographed. All experiments were repeated at least three times with identical results. **h** Chlorophyll content in seedlings after 5 μM MV treatment. **b–e, h** Each column represents an average of three replicates, and bars indicate SDs. ** and * indicate significant differences relative to the control at *P* < 0.01 and *P* < 0.05, respectively

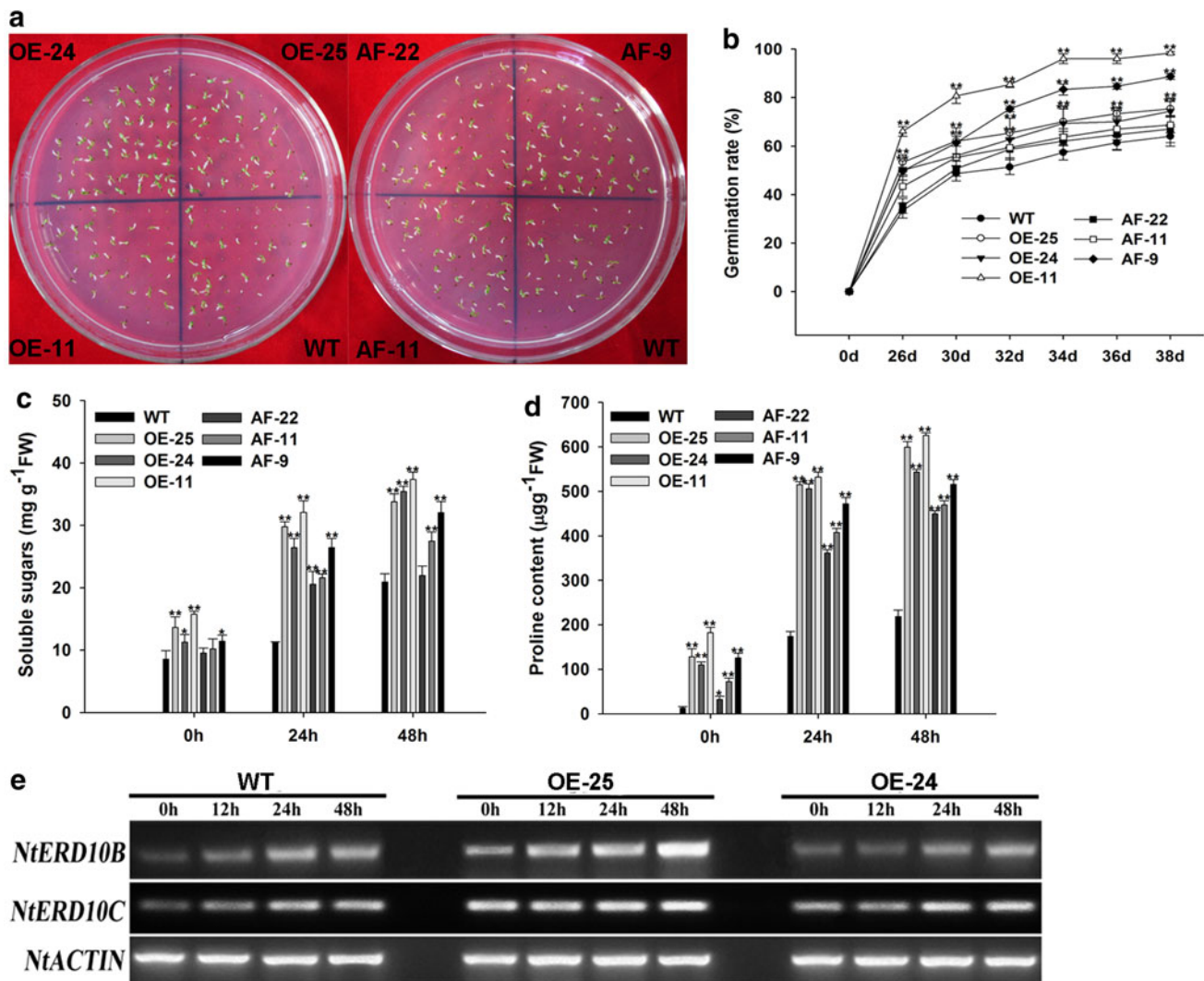


Fig. 6 Low temperature tolerance of transgenic and WT tobacco plants. **a** Transgenic and WT tobacco seed germination rate under low temperature stress (8°C). The seeds were allowed to grow for 38 days before the photographs were taken. **b** Germination rate under low temperature stress (8°C). Germination rate (root emergence) was evaluated at indicated time after sowing. Soluble sugars **c** and proline concentrations **d** in 6-week-old transgenic and WT tobacco plants before and after low temperature treatment (4°C) for indicated time.

b–d Each column represents the average of three replicates, and *bars* indicate SDs. ** and * indicate significant differences relative to the control at $P < 0.01$ and $P < 0.05$, respectively. **e** Expression of stress-related genes by RT-PCR. Total RNA was extracted from leaf samples at the indicated times after 4°C treatment. All RT-PCR reactions were from the same batch of cDNA and repeated at least four times with identical results

growth (Fig. 7d). No symptoms were observed in the plants inoculated with control serum.

Enhanced disease resistance in plants is often associated with the specific induction of elaborate defense-signaling pathways. The major players that regulate the signaling pathways include the plant hormones SA, JA, and ethylene (Kachroo and Kachroo 2007). In order to reveal the potential reasons for enhanced pathogen resistance in the OE plants, the expression levels of four marker genes from different pathways (PR1a and PR5 for SA signaling, PR4 for MeJA signaling, and EREBP for ethylene signaling) were determined (Shi et al. 2010). As shown in Fig. 8, after

inoculation with PVY, PR1a was induced earlier (within 1 day) and stronger in the OE plants than in the WT and AF lines, but there was no significant change in PR5 expression. PR4 was only induced in the OE lines at 4 and 6 days after infection. Before infection, EREBP had a higher transcription level in the OE lines than in the WT or AF lines. However, the expression of EREBP was almost completely suppressed in all lines by PVY inoculation. Thus, the constitutive overexpression of *ZmMPK17* appears to enhance resistance to CMV and PVY, probably because the expression of many PR genes is elevated, and the kinase activity is required for viral resistance.

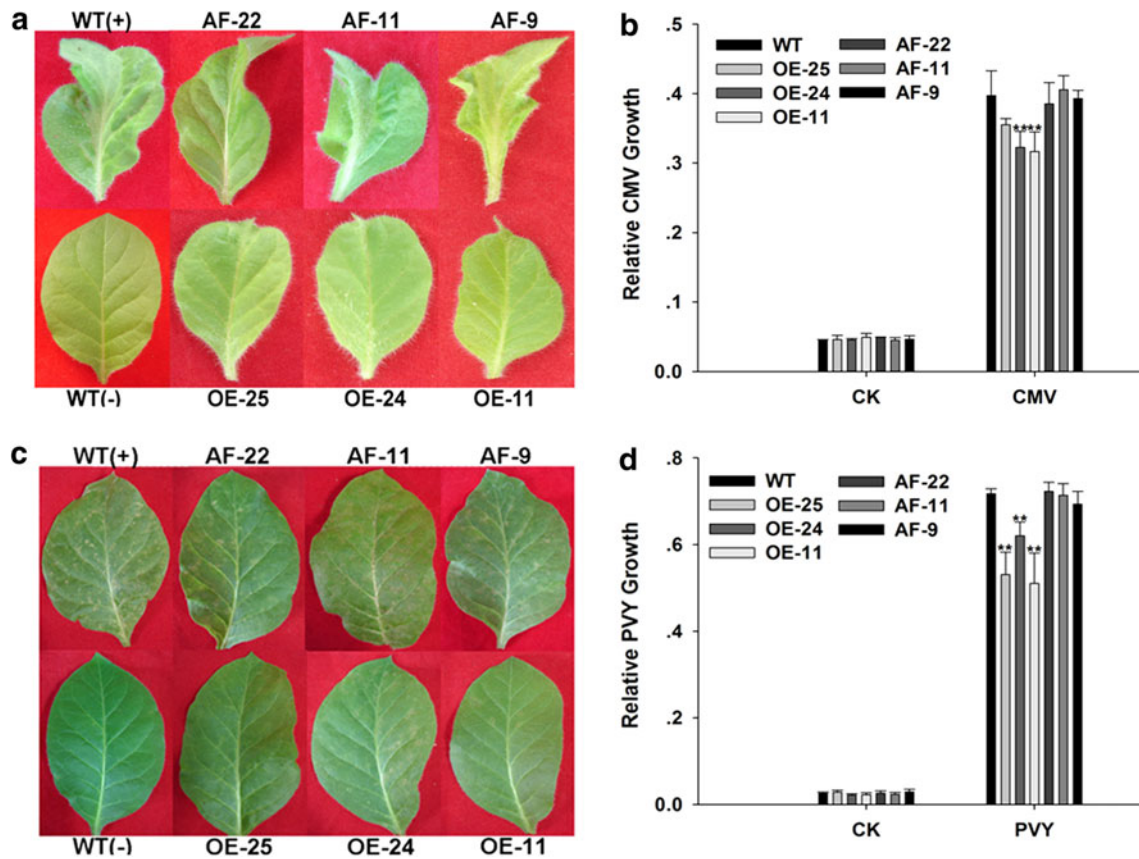


Fig. 7 Enhanced viral resistance against CMV and PVY in WT and transgenic plants. **a** Phenotype of the seventh true leaves of tobacco inoculated with CMV at 15 days. WT(–): mock inoculation. **c** Symptoms of the sixth true leaves of tobacco inoculated with PVY at 30 days. **b, d** Virus accumulation was determined by ELISA

and relative virus growth was indicated by absorbance at 492 nm. CK: mock inoculation. **b, d** Each column represents the average of three replicates, and *bars* indicate SDs. ** and * indicate significant differences relative to the control at $P < 0.01$ and $P < 0.05$, respectively

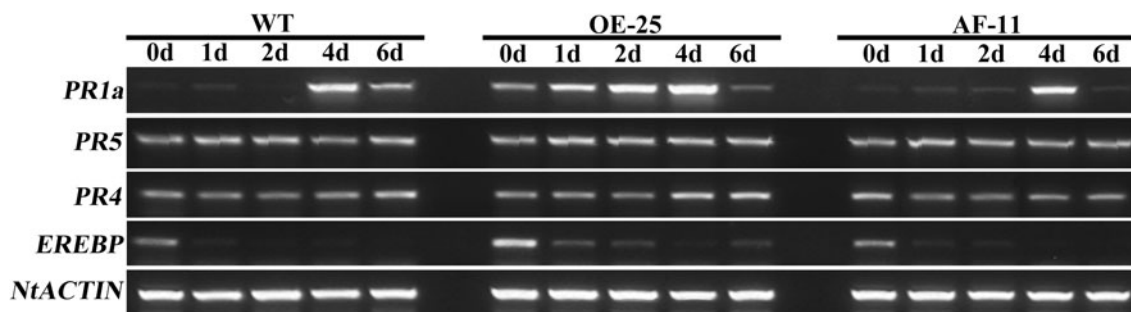


Fig. 8 Expression of PR genes by RT-PCR after inoculation with PVY Total RNA was extracted from the sixth true leaves at indicated times. All RT-PCR reactions were from the same batch of cDNA and were repeated at least four times with identical results

Discussion

Several group D MAPKs have been characterized in rice in terms of their expression patterns and potential roles in biotic and abiotic stress tolerance. *OsBWMK1* was induced by *Magnaprote grisea*, defense-signaling molecules and abiotic stresses including salt, drought, increased temperature (37°C), heavy metals etc. (Cheong et al. 2003).

OsBIMK2 was activated by benzothiadiazole (BTH) treatment and further upregulated with subsequent *M. grisea* inoculation (Song et al. 2006). Overexpression of *OsBWMK1* or *OsBIMK2* in transgenic tobacco caused enhanced disease resistance. Expression of *OsWJUMK1*, which has a strong baseline expression in untreated healthy leaves, was slightly upregulated by ABA, H₂O₂, drought and 12°C, and greatly upregulated by heavy metals, low

temperature and *M. grisea* infection (Agrawal et al. 2003). In this study, we examined the response of *ZmMPK17* to PEG, low temperature and defense-signaling molecules such as ABA, SA, JA, ethylene and H_2O_2 (Fig. 3); this expression pattern occurs in response to various stress stimuli and is similar to group D MAPKs in rice. This suggests that they may serve similar functions.

In the present study, transient expression of the *ZmMPK17*-GFP fusion protein in onion epidermal cells indicated that *ZmMPK17* is localized in the nucleus (Fig. 2), the same organelle into which MAPKs are translocated upon activation. Stimulus-induced activation of MAPKs correlates with dynamic changes in their localization, whereby the proteins often translocate to and accumulate in the nucleus. This has been shown to be true of *Arabidopsis* MPK3 and MPK6 after ozone treatment of parsley (*Petroselinum crispum*) PcMPK3 and PcMPK6 after elicitation and of peanut (*Arachis hypogaea*) AhMPK3 after exposure to H_2O_2 (Ahlfors et al. 2004; Lee et al. 2004; Kumar et al. 2009). This is often required due to the nuclear localization of key MAPK substrates, including transcription factors involved in the control of gene expression (Mutalik and Venkatesh 2006). The CD of *ZmMPK17* was found to be essential for nuclear localization. This was also observed for OsBWMK1. The CD of BWMK1, which contains a putative leucine zipper motif, is believed to be essential for its targeting to the nucleus (Cheong et al. 2003). Thus, it is reasonable to speculate that *ZmMPK17* may phosphorylate transcription factors that in turn regulate gene expression in plants.

The double-peaking of *ZmMPK17* expression under SA and MeJA treatments might suggest existence of positive amplification loops in SA and MeJA signaling. This has also been reported in ROS signaling in response to elicitor and oxidative stress (Yoshioka et al. 2003; Rizhsky et al. 2004). ABA induced H_2O_2 production was shown to activate MAPK, which in turn induces the expression and the activities of antioxidant enzymes (Zhang et al. 2006). The activation of MAPK also enhances the H_2O_2 production, forming a positive feedback loop (Zhang et al. 2006). Recent studies have suggested that *ZmMPK5* activated by brassinosteroids-induced apoplastic H_2O_2 accumulation induces NADPH oxidase gene expression, which in turn enhances H_2O_2 accumulation and BR signaling in leaves of maize plants (Zhang et al. 2010).

As shown in Fig. 3b, k, the transcription level of *ZmMPK17* was gradually suppressed after PEG treatment, whereas *ZmMPK17*-overexpressing plants showed enhanced osmotic stress tolerance through ROS scavenging. Overexpression of signaling elements, especially in the heterologous overexpression system, has been reported to non-specifically perturb signal transduction in other plants. For example, *OsMPK6* suppression enhances rice resistance

to bacterial blight, whereas small number of *OsMPK6*-overexpressing plants also show enhanced *Xoo* resistance when they developed lesion mimics on their leaves (Yuan et al. 2007; Shen et al. 2010). Further studies are needed to determine what molecular mechanisms increase osmotic stress tolerance of *ZmMPK17*-overexpressing plants.

Plants have developed sophisticated systems to protect themselves from oxidative stress by adjusting ROS homeostasis. These systems include numerous scavenging enzymes such as superoxide dismutase (SOD), POD, APX, glutathione peroxidase, and CAT (Apel and Hirt 2004). When cellular ROS levels are low, they act as signaling molecules. Under serious biotic and abiotic stress, ROS can be overproduced and damage cell growth (Mittler et al. 2004). MAPK cascades are key players in ROS signaling. Several studies have shown that MAPK signaling pathways are not only induced by ROS but also can regulate ROS production (Pitzschke and Hirt 2009).

Exogenous H_2O_2 has been shown to activate various *Arabidopsis* MAPK cascades, including MPK3/MPK6/MPK4. AtMKK1–AtMPK6 regulate H_2O_2 metabolism through CAT1. CAT2 expression seems to be regulated by the MEKK1–MPK4 cascade (Rodriguez et al. 2010). More recently, Ning et al. (2010) reported that drought hypersensitivity of *dsm1* (a MAPKKK) is partially due to a decrease in ROS scavenging. The transcription levels of *POX22.3* and *POX8.1* were significantly lower in the mutants than in the WT under both normal and drought stress conditions. In the present study, we demonstrated that H_2O_2 -mediated PEG induced the expression of *ZmMPK17* and that *ZmMPK17*-overexpressing tobacco plants showed enhanced ability of ROS scavenging, which may have resulted from increased transcription levels of *NtAPX* and *NtCAT1* and increased APX and CAT activities. These findings imply that *ZmMPK17* mediates oxidative stress responses and is not only induced by ROS but also regulate ROS levels by affecting antioxidant defense systems.

In the cold stress assay, the germination rate of the OE and AF lines was significantly higher than that of the WT lines. The higher levels of proline and soluble sugars in six transgenic lines may have contributed to enhanced cold tolerance. The kinase activity of *ZmMPK17* was not essential for its function in response to cold stress. Previous studies have shown that induction of the expression of *SIPK* and the (*W/S*)*IPK* chimera leads to HR-like cell death. (*W/S*)*IPK* is constructed chimera with a *WIPK* N-terminus fused to a *SIPK* C-terminus. This result suggests that the C-terminus of *SIPK* contains the molecular determinant for its activity (Zhang and Liu 2001). *ZmMPK17* have a C-terminal region extension, which is not seen in other plant MAPKs (Fig. 1a). This C-terminal region may play an important role in its response to cold stress, but this hypothesis requires future research.

Treatment with exogenous SA, JA and ethylene increased the expression of *ZmMPK17* in maize seedlings (Fig. 3), indicating that *ZmMPK17* may be involved in SA/JA/ethylene-dependent defense responses and in the regulation of certain components of multiple stress-signaling pathways. In *Arabidopsis*, H₂O₂ activates the MKK3–MPK7 module, which induces target genes, such as PR1 and therefore activates the defense responses (Doczi et al. 2007). OsBWMK1 may mediate SA-dependent defense responses by activating the WRKY transcription factor in plants (Koo et al. 2009). Suppressing *OsMPK6* expression influences the transcription levels of a subset of defense-related genes and the level of endogenous salicylic acid (Yuan et al. 2007). Overexpression of *GhMPK7* confers enhanced resistance to fungi and viruses in transgenic plants, and the transcript levels of SA-pathway genes are more rapidly and strongly induced (Shi et al. 2010). Like *GhMPK7*, *ZmMPK17* might be involved in SA-mediated pathogen defense-signaling pathways. To support this theory, we created transgenic tobacco plants that overexpressed *ZmMPK17* under the control of the CaMV 35S promoter. Significantly, the plants had higher levels of *PR1a* and *EREBP* expression and an enhanced resistance to viral pathogens (Figs. 7, 8). *PR1a* is known as a marker gene for the SA signaling pathway, but the expression of the ethylene pathway marker gene *EREBP* was almost completely suppressed after PVY inoculation. Therefore, we speculate that *ZmMPK17* may act as a positive regulator of SA and ethylene-dependent defense. Although the SA- and JA/ethylene-defense pathways are mutually antagonistic, evidence of synergistic interactions have also been reported (Bari and Jones 2009). Mur et al. (2006) reported that there was a transient synergistic enhancement in the expression of genes associated with either JA (PDF1.2 and Thi1.2) or SA (*PR1*) signaling when both substances were applied at low concentrations.

In this study, a novel group D MAPK gene *ZmMPK17* was identified and characterized. We established that *ZmMPK17* is involved in response to PEG, low temperature, and defense-signaling molecules. Overexpression of *ZmMPK17* in transgenic tobacco plants resulted in enhanced tolerance to cold stress and viral infection. The transgenic tobacco plants exhibited enhanced ROS scavenging ability due to upregulation of the expression of various oxidative stress-related genes under osmotic stress conditions. *ZmMPK17* may serve as a cross-talk point between biotic and abiotic stress responses. These findings not only extend our knowledge of the biologic function of group D MAPKs but also provide new insights for further exploration of the significance of *ZmMPK17* in the regulation of plant defense responses. Further work at the protein level is needed to provide detailed data on this regulatory mechanism.

Acknowledgments We thank Lin Ma (Shandong Agricultural University, P.R.China) for providing pathogen and polyclonal anti-serum for CMV and PVY detection. Funding for this research was provided by the Grants from the National Natural Science Foundation of China (Nos.30871457 and 31071337) and the State Key Basic Research and Development Plan of China (No.2009CB118500).

References

- Agrawal GK, Agrawal SK, Shibato J, Iwahashi H, Rakwal R (2003) Novel rice MAP kinases OsMSRMK3 and OsWJUMK1 involved in encountering diverse environmental stresses and developmental regulation. *Biochem Biophys Res Commun* 300:775–783
- Ahlfors R, Macioszek V, Rudd J, Brosche M, Schlichting R, Scheel D, Kangasjarvi J (2004) Stress hormone-independent activation and nuclear translocation of mitogen-activated protein kinases in *Arabidopsis thaliana* during ozone exposure. *Plant J* 40:512–522
- Alexandrov NN, Brover VV, Freidin S, Troukhan ME, Tatarinova TV, Zhang H, Swaller TJ, Lu YP, Bouck J, Flavell RB, Feldmann KA (2009) Insights into corn genes derived from large-scale cDNA sequencing. *Plant Mol Biol* 69:179–194
- Apel K, Hirt H (2004) Reactive oxygen species: metabolism, oxidative stress, and signal transduction. *Annu Rev Plant Biol* 55:373–399
- Bari R, Jones JD (2009) Role of plant hormones in plant defence responses. *Plant Mol Biol* 69:473–488
- Cheong YH, Moon BC, Kim JK, Kim CY, Kim MC, Kim IH, Park CY, Kim JC, Park BO, Koo SC, Yoon HW, Chung WS, Lim CO, Lee SY, Cho MJ (2003) BWMK1, a rice mitogen-activated protein kinase, locates in the nucleus and mediates pathogenesis-related gene expression by activation of a transcription factor. *Plant Physiol* 132:1961–1972
- Colcombet J, Hirt H (2008) *Arabidopsis* MAPKs: a complex signaling network involved in multiple biological processes. *Biochem J* 413:217–226
- Couee I, Sulmon C, Gouesbet G, El Amrani A (2006) Involvement of soluble sugars in reactive oxygen species balance and responses to oxidative stress in plants. *J Exp Bot* 57:449–459
- Doczi R, Brader G, Pettko-Szandtner A, Rajh I, Djamei A, Pitzschke A, Teige M, Hirt H (2007) The *Arabidopsis* mitogen-activated protein kinase kinase MKK3 is upstream of group C mitogen-activated protein kinases and participates in pathogen signaling. *Plant Cell* 19:3266–3279
- Duerr B, Gawienowski M, Ropp T, Jacobs T (1993) MsERK1: a mitogen-activated protein kinase from a flowering plant. *Plant Cell* 5:87–96
- Heckman KL, Pease LR (2007) Gene splicing and mutagenesis by PCR-driven overlap extension. *Nat Protoc* 2:924–932
- Irigoyen JJ, Emerich DW, Sanchez-Diaz M (1992) Water stress induced changes in concentrations of proline and total soluble sugars in nodulated alfalfa (*Medicago sativa*) plants. *Physiol Plant* 84:55–60
- Jiang M, Zhang J (2001) Effect of abscisic acid on active oxygen species, antioxidative defence system and oxidative damage in leaves of maize seedlings. *Plant Cell Physiol* 42:1265–1273
- Kachroo A, Kachroo P (2007) Salicylic acid-, jasmonic acid- and ethylene-mediated regulation of plant defense signaling. *Genet Eng* 28:55–83
- Kasuga M, Miura S, Shinozaki K, Yamaguchi-Shinozaki K (2004) A combination of the *Arabidopsis* DREB1A gene and stress-inducible rd29A promoter improved drought- and low-temperature stress tolerance in tobacco by gene transfer. *Plant Cell Physiol* 45:346–350

- Ko CH, Brendel V, Taylor RD, Walbot V (1998) U-richness is a defining feature of plant introns and may function as an intron recognition signal in maize. *Plant Mol Biol* 36:573–583
- Koo SC, Moon BC, Kim JK, Kim CY, Sung SJ, Kim MC, Cho MJ, Cheong YH (2009) OsBWMK1 mediates SA-dependent defense responses by activating the transcription factor OsWRKY33. *Biochem Biophys Res Commun* 387:365–370
- Kumar KR, Srinivasan T, Kirti PB (2009) A mitogen-activated protein kinase gene, *AhMPK3* of peanut: molecular cloning, genomic organization, and heterologous expression conferring resistance against *Spodoptera litura* in tobacco. *Mol Genet Genomics* 282:65–81
- Lalle M, Visconti S, Marra M, Camoni L, Velasco R, Aducci P (2005) ZmMPK6, a novel maize MAP kinase that interacts with 14-3-3 proteins. *Plant Mol Biol* 59:713–722
- Lee J, Rudd JJ, Macioszek VK, Scheel D (2004) Dynamic changes in the localization of MAPK cascade components controlling pathogenesis-related (PR) gene expression during innate immunity in parsley. *J Biol Chem* 279:22440–22448
- Liu Q, Xue Q (2007) Computational identification and phylogenetic analysis of the MAPK gene family in *Oryza sativa*. *Plant Physiol Biochem* 45:6–14
- Liu L, Hu X, Song J, Zong X, Li D, Li D (2009) Over-expression of a *Zea mays* L. protein phosphatase 2C gene (*ZmPP2C*) in *Arabidopsis thaliana* decreases tolerance to salt and drought. *J Plant Physiol* 166:531–542
- MAPK Group (2002) Mitogen-activated protein kinase cascades in plants: a new nomenclature. *Trends Plant Sci* 7:301–308
- Mishra NS, Tuteja R, Tuteja N (2006) Signaling through MAP kinase networks in plants. *Arch Biochem Biophys* 452:55–68
- Mittler R, Vanderauwera S, Gollery M, Van Breusegem F (2004) Reactive oxygen gene network of plants. *Trends Plant Sci* 9:490–498
- Mur LA, Kenton P, Atzorn R, Miersch O, Wasternack C (2006) The outcomes of concentration-specific interactions between salicylate and jasmonate signaling include synergy, antagonism, and oxidative stress leading to cell death. *Plant Physiol* 140:249–262
- Mutalik VK, Venkatesh KV (2006) Effect of the MAPK cascade structure, nuclear translocation and regulation of transcription factors on gene expression. *Biol Systems* 85:144–157
- Ning J, Li X, Hicks LM, Xiong L (2010) A Raf-like MAPKKK gene *DSM1* mediates drought resistance through reactive oxygen species scavenging in rice. *Plant Physiol* 152:876–890
- Pitzschke A, Hirt H (2009) Disentangling the complexity of mitogen-activated protein kinases and reactive oxygen species signaling. *Plant Physiol* 149:606–615
- Pitzschke A, Schikora A, Hirt H (2009) MAPK cascade signaling networks in plant defence. *Curr Opin Plant Biol* 12:421–426
- Reyna NS, Yang Y (2006) Molecular analysis of the rice MAP kinase gene family in relation to *Magnaporthe grisea* infection. *Mol Plant Microbe Interact* 19:530–540
- Rizhsky L, Davletova S, Liang H, Mittler R (2004) The zinc finger protein Zat12 is required for cytosolic ascorbate peroxidase 1 expression during oxidative stress in *Arabidopsis*. *J Biol Chem* 279:11736–11743
- Rodriguez MC, Petersen M, Mundy J (2010) Mitogen-activated protein kinase signaling in plants. *Annu Rev Plant Biol* 61:621–649
- Seo S, Sano H, Ohashi Y (1999) Jasmonate-based wound signal transduction requires activation of WIPK, a tobacco mitogen-activated protein kinase. *Plant Cell* 11:289–298
- Shen X, Yuan B, Liu H, Li X, Xu C, Wang S (2010) Opposite functions of a rice mitogen-activated protein kinase during the process of resistance against *Xanthomonas oryzae*. *Plant J* 64:86–99
- Shi J, An HL, Zhang L, Gao Z, Guo XQ (2010) *GhMPK7*, a novel multiple stress-responsive cotton group C MAPK gene, has a role in broad spectrum disease resistance and plant development. *Plant Mol Biol* 74:1–17
- Song D, Chen J, Song F, Zheng Z (2006) A novel rice MAPK gene, *OsBIMK2*, is involved in disease-resistance responses. *Plant Biol* 8:587–596
- Teige M, Scheikl E, Eulgem T, Doczi R, Ichimura K, Shinozaki K, Dangl JL, Hirt H (2004) The MKK2 pathway mediates cold and salt stress signaling in *Arabidopsis*. *Mol Cell* 15:141–152
- Tena G, Asai T, Chiu WL, Sheen J (2001) Plant mitogen-activated protein kinase signaling cascades. *Curr Opin Plant Biol* 4:392–400
- Walia A, Lee JS, Wasteneys G, Ellis B (2009) *Arabidopsis* mitogen-activated protein kinase MPK18 mediates cortical microtubule functions in plant cells. *Plant J* 59:565–575
- Wang M, Zhang Y, Wang J, Wu X, Guo X (2007) A novel MAP kinase gene in cotton (*Gossypium hirsutum* L.), GhMAPK, is involved in response to diverse environmental stresses. *J Biochem Mol Biol* 40:325–332
- Yoshioka H, Numata N, Nakajima K, Katou S, Kawakita K, Rowland O, Jones JDG, Doke N (2003) *Nicotiana benthamiana* gp91^{phox} homologs *NbrbohA* and *NbrbohB* participate in H₂O₂ accumulation and resistance to *Phytophthora infestans*. *Plant Cell* 15:706–718
- Yoshioka H, Mase K, Yoshioka M, Kobayashi M, Asai S (2010) Regulatory mechanisms of nitric oxide and reactive oxygen species generation and their role in plant immunity. *Nitric Oxide* 25:216–221
- Yuan B, Shen X, Li X, Xu C, Wang S (2007) Mitogen-activated protein kinase OsMPK6 negatively regulates rice disease resistance to bacterial pathogens. *Planta* 226:953–960
- Zhang S, Liu Y (2001) Activation of salicylic acid-induced protein kinase, a mitogen-activated protein kinase, induces multiple defense responses in tobacco. *Plant Cell* 13:1877–1889
- Zhang S, Du H, Klessig DF (1998) Activation of the tobacco SIP kinase by both a cell wall-derived carbohydrate elicitor and purified proteinaceous elicitors from *Phytophthora* spp. *Plant Cell* 10:435–450
- Zhang A, Jiang M, Zhang J, Tan M, Hu X (2006) Mitogen-activated protein kinase is involved in abscisic acid-induced antioxidant defense and acts downstream of reactive oxygen species production in leaves of maize plants. *Plant Physiol* 141:475–487
- Zhang A, Zhang J, Ye N, Cao J, Tan M, Zhang J, Jiang M (2010) ZmMPK5 is required for the NADPH oxidase-mediated self-propagation of apoplastic H₂O₂ in brassinosteroid-induced antioxidant defence in leaves of maize. *J Exp Bot* 61:4399–4411
- Zhang L, Xi D, Luo L, Meng F, Li Y, Wu CA, Guo X (2011) Cotton GhMPK2 is involved in multiple signaling pathways and mediates defense responses to pathogen infection and oxidative stress. *FEBS J* 278:1367–1378
- Zhu JK (2002) Salt and drought stress signal transduction in plants. *Annu Rev Plant Biol* 53:247–273
- Zong XJ, Li DP, Gu LK, Li DQ, Liu LX, Hu XL (2009) Abscisic acid and hydrogen peroxide induce a novel maize group C MAP kinase gene, *ZmMPK7*, which is responsible for the removal of reactive oxygen species. *Planta* 229:485–495